J Mater Sci (2011) 46:6682–6689
DOI 10.1007/s10853-011-5621-6

Hydrophobic properties and color effects of hybrid silica spin-coatings on cellulose matrix

Yunjie Yin · Chaoxia Wang · Chunxia Wang · Min Wu · Anli Tian · Shaohai Fu

Received: 5 April 2011 / Accepted: 9 May 2011 / Published online: 7 June 2011

Abstract A novel sol–gel derived organic–inorganic hybrid silica sol consisting of organic direct red dye 4BS and inorganic silica (SiO_2) is successfully synthesized by adding coupling agent γ-chloropropyltriethoxysilane (CPTS). Hybrid silica coatings are deposited on cellulose matrix surface via spin-coating approach to introduce effective hydrophobic and color properties. Compared to the dye hybrid silica sol (DHSS), the particle size of CPTS/dye hybrid silica sol (CDHSS) increases from 64.51 to 129.70 nm, while the surface tension reduces from 34.27×10^{-3} N m^{-1} to 31.22×10^{-3} N m^{-1}. The hydrostatic pressure of the cellulose matrix coating with CDHSS is 4530.5 Pa, the contact angle is 131.48°, and the wetting time is ~150 min, which attributes to the alkyl chloride aliphatic chain and sharp micro-surface roughness of the hybrid coatings validated directly by AFM and SEM images. The *K*/*S* value (5.15) of the cellulose matrix coated with CPTS/dye hybrid silica (CMCCDHS) is 12.44% higher than that of the cellulose matrix coated with dye hybrid silica (CMCDHS), and increased by 30.38% relative to the control coated sample. The maximum absorption wavelengths of the matrixes treated with different processes are the same as the maximum absorption wavelength of the silica sols (510 nm).

Introduction

The sol–gel process provides very attractive pathways to develop hybrid materials in which active species are embedded to form inorganic or organic–inorganic networks [1–4]. The recent research work about sol–gel inorganic material used as solid host for laser dye materials has attracted much attention due to its high potential utility compared to polymers. The conventional inorganic material production, such as glass and ceramic, requires high temperature at which laser dyes cannot withstand. Whereas, the sol–gel reaction usually occurs at low temperature (<60 °C), and organic dye molecules can be incorporated in the gel networks with no risk of thermal degradation [5, 6]. Therefore, the sol–gel technique is a novel way for doping organic dye molecules into inorganic silica host [7, 8]. Various procedures are utilized to incorporate the laser dyes into sol–gel matrixes, such as doping or dipping methods [9].

A problem encountered in the preparation of silica gel is crack and fracture formation, and this usually occurs during the drying process. Crack and fracture are mainly due to the unstable temperature and pressure gradients during the heating process [10, 11]. Another reason of crack and fracture is the vulnerable hydrolysis oxane bonds (Si–O–Si). Some researches demonstrated that silica coupling agents could improve the compatibility of dyes and SiO_2 hybrid materials, and minimize the phase separation [12–15]. The mechanical and hydrophobic properties of silica gel are improved via the silica coupling agent monomer for the unique structure in the copolymeric gel [16, 17].

Sol–gel hybrid materials impart transparence and soft coatings to cellulose fabrics [18, 19]. By doping the function materials into the matrix sol [20, 21] and spin-coating the fabric, thin hybrid coatings are formed on the cellulose matrixes, and many special properties are generated on the fibers [22, 23]. The function materials including repellent agent CPTS also dope into the matrix sol, and the properties of sol–gel hybrids materials are

Y. Yin · C. Wang (✉) · C. Wang · M. Wu · A. Tian · S. Fu
Key Laboratory of Eco-Textile, Ministry of Education, Jiangnan University, 1800 Lihu Road, Wuxi 214122, China
e-mail: wangchaoxia@sohu.com

presented on the cellulose matrixes [24]. CPTS, because of its well-defined organic–inorganic phase segregation at nanometer scale, effectively prevents the aggregation of direct dyes at a relatively higher concentration. And the CPTS plays a shielding role in protecting the chromophore from quenching due to other activated species like molecular oxygen and ultraviolet ray [25].

This research concerns that CPTS/dye hybrid silica sol (CDHSS), prepared by doping direct red dye 4BS and silica coupling agent CPTS, was spin-coated on the cellulose matrix. The hydrophobicity and chromatometry of CMCDHS and CMCCDHS were investigated via analyzing the particle size, surface tension, contact angle of water, hydrostatic pressure, *K*/*S* value, etc.

Experimental

Materials

The cellulose matrix–poplin 100% cotton woven fabric weighting 141.0 g m^{-2} was used, which was produced by Jiangsu Hongdou Industrial Co., Ltd (China). The tetraethoxysilane (TEOS, Mw 208.33), ethyl alcohol (EtOH, 99.7%), and HCl (37.0%) were purchased from Sinopharm Chemical Reagent Co., Ltd (China). The γ-chloropropyltriethoxysilane (CPTS, Mw 240.79) was obtained by Hubei Jianghan Chemical Co., Ltd (China). All the chemicals are analytical reagent grade. The direct red dye 4BS (C.I. Direct Red 23, Mw 813.72, Orichem International Ltd) was used in this research and it is technical grade. The molecular structures of direct red dye 4BS and CPTS are shown in Schemes 1 and 2.

Preparation of silica sols

The CDHSS was prepared by adding EtOH, TEOS, H_2O, and CPTS (TEOS:H_2O:EtOH:CPTS = 1:5:6:0.2; Molar ratio) in a rotating erlenmeyer flask. The mixture (94.20 mL) was stirred at room temperature for 25 min with a magnetic stirring apparatus (800 rpm), and then pH value was adjusted to 3.50 with HCl (1 mol L^{-1}, approximately 0.80 mL). 5 mL direct red dye 4BS solution (10%, mass concentration) was added into the mixture. The sol was obtained after stirred at 50 °C for 6 h and aged for 24 h [26].

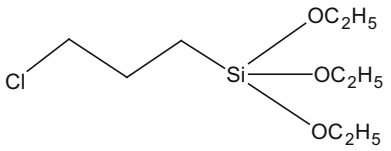

Scheme 2 Molecular structure of CPTS (CAS No: 5089-70-3)

The dye hybrid silica sol (DHSS) was prepared similarly as above process, and the quotient of CPTS was replaced by EtOH. Another control dye solution was prepared by mixing direct dye and H_2O with the same dye concentration as the silica solution mentioned previously.

Spin-coating on cellulose matrix

The cellulose matrix was pre-cleared in deionized water and fixed onto the rotor of KW-4A spincoater (Chemat Technology, Inc. USA). 20 g silica sol was dropped onto the cellulose matrix at the speed of 800 rpm in 10 s. Then the rotor was sped up to 4,000 rpm and coated for 50 s [27]. The coated cellulose matrix sample was dried at 60 °C for 20 min and finally cured at 150 °C for 3 min with a thermal annealing speed of 3 °C min^{-1}.

Particle size measurement

The particle size distribution of the sol was measured via Nano-ZS90 Zetasizer Nano series supplied by Malvern Instruments Ltd (UK). The silica dish containing 2 mL silica sol was laid in the sample room at 25 °C. The scanning data and particle size distribution curve were analyzed by DTS software.

Surface tension and contact angle measurement

The surface tension was measured by the Wilhelmy Plate method and Du Noüy Ring method using the KRÜSS DSA100 Drop Shape Analysis System (KRÜSS GmbH, Germany) at 25 °C [28, 29]. The surface tension was recorded when the water drop is the largest below the sample pinhole (Fig. 1).

The contact angle and the wetting time were measured also using the KRÜSS DSA100 Drop Shape Analysis System. The contact angle values were recorded when the water drop stilled on the cellulose matrixes. A water drop was recorded every 10 min, and when the contact angle was 0, the

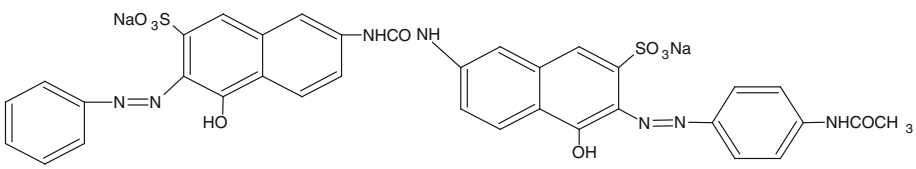

Scheme 1 Molecular structure of direct red dye 4BS (C.I. Direct Red 23)

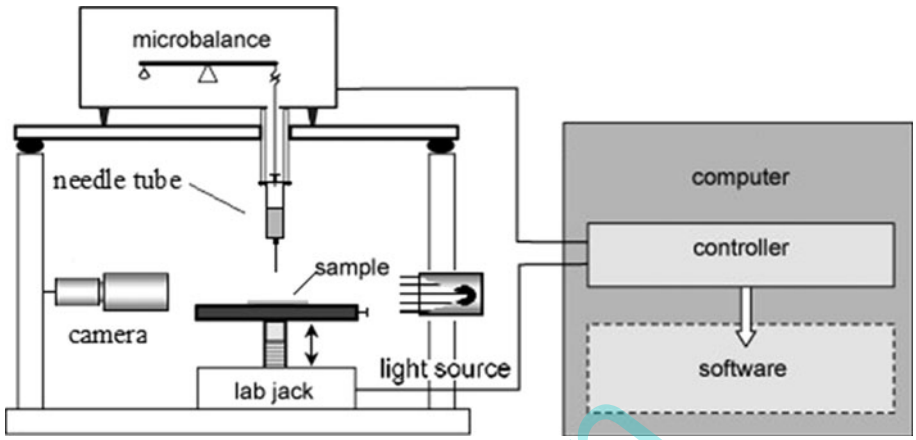

Fig. 1 A schematic of the modified Wilhelmy apparatus used for the determination of the surface tension and contact angle of fabric matrixes

recorded time just was the wetting time [30]. The experiments were carried out at 25 °C and 40% relative humidity.

Hydrostatic pressure measurement

The hydrostatic pressure reflects the water repellent and hydrophobicity of the matrix. With lower surface free energy and thicker deposition, matrix has a larger hydrostatic pressure. According to AATCC-127-2008, treated matrix is conditioned at 25 °C and 65% relative humidity for 4 h. The relative height of the water column is recorded when the water drops exudes in three different places from the matrix. The pressure is equal to the relative height of the water column. The hydrostatic pressure values are obtained by the formula:

$$P\ (\mathrm{Pa}) = \rho g h, \tag{1}$$

where h is the height of hydrostatic pressure (m), ρ is the density of H_2O and usually it is 1.0×10^3 kg m^{-3}, g is the acceleration of gravity (m s^{-2}), and the value of the acceleration of gravity is most accurately known as 9.8 m s^{-2}. Five pressure readings are taken from each matrix, and the average value is recorded.

Color measurement

The color properties of the samples were determined with an Xrite-8400 spectrophotometer obtained from America X-Rite Co., Ltd, under the illuminant D65 using the 10° standard observer. The K/S, L^*, a^*, b^*, h^*, and E values were gained, which showed the color performances of the matrix. The three coordinates of CIELAB represent the lightness of the color (L^*, $L^* = 0$ yields black and $L^* = 100$ indicates white), its position between red and green (a^*, negative values indicate green, while positive values indicate magenta), and between yellow and blue (b^*, negative values indicate blue, while positive values indicate yellow):

$$K/S = \frac{(1-R)^2}{2R}, \tag{2}$$

where K is the absorption coefficient, S is the scattering coefficient, and R is the fractional reflectance (value from 0 to 1) of color matrix at the wavelength of minimum reflectance [31].

Atomic force microscopy measurement

The topography of the silica sol coatings on mica sheet was investigated by atomic force microscopy (AFM) at 25 °C and 40% relative humidity using a CSPM4000 AFM made by Benyuan Co, Ltd (China) operating in contact mode. The tip is slowly scanned across the surface of the coatings. The force between the atoms on the surface of the scanned material and those on the scanning tip lead to the tip to deflect. This deflection is recorded using a laser focused on the top of the cantilever and reflected onto photodetector. The photodetector signals are used to map the surface characteristics of specimens with resolutions down to the nanoscale [32].

Scanning electron microscope measurement

The scanning electron microscope (SEM) photographs of coated matrix were tested by a JSM-5610 scanning electron micro-scope (JEOL Ltd, Tokyo, Japan) under 5000× magnifications. The cellulose matrixes dried and sputter coated with gold using a current of 10 mA.

Results and discussion

Particle size of silica sols

Figure 2 shows the particle size distribution comparison of DHSS and CDHSS. According to Fig. 2, the particle sizes

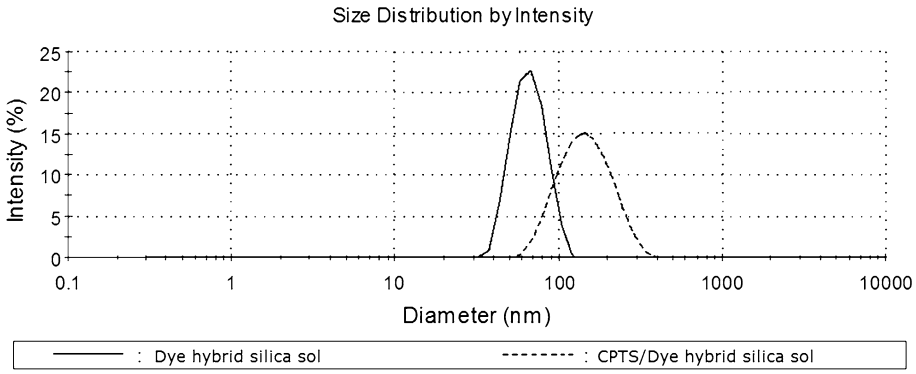

Fig. 2 Particle size distribution of silica sols

of the DHSS are in an average size of 64.5 nm, while the particle size of CDHSS increases to 129.7 nm. Although the particle sizes of CDHSS are more than doubled to the one without CPTS, the colloidal dispersion of CDHSS is stable. From Fig. 2, the distribution range of the CDHSS is between 58.0 and 385.0 nm, and the distribution range of the DHSS is between 31.0 and 132.0 nm. This indicates that the particle size of CDHSS is more widely distributed and will introduce a rougher surface after gelation.

Surface tension of silica sols

Surface tension of silica sol is closely related to the hydrophobicity and wetting property of the matrix. The surface-free energy of cellulose matrix is about 200×10^{-3} N m^{-1}. During the coating process, sol drops with lager surface tension easily roll down from the cellulose matrix, so the silica coating becomes thinner and the dye on the cellulose matrix is less, while sol drops with lower surface tension easily wet the cellulose matrix, and the dye in the silica sol is adsorbed more easily to the cellulose matrix, which may bring to a larger color strength (*K*/*S* value). From Fig. 3, the surface tension of the control dye solution is 98.34×10^{-3} N m^{-1} and the surface tension of the DHSS is 34.27×10^{-3} N m^{-1}. After doping CPTS, the surface tension decreases to 31.22×10^{-3} N m^{-1} mainly for the long alkyl chloride aliphatic chain of coupling agent. During gelling, the ethanol is easily evaporated, and then it has less effect on the surface-free energy of the cellulose matrix. Nevertheless, the CPTS can bond with the silica coatings, and it affects the surface-free energy of the cellulose matrix, which leads to a further decrease of the surface tension.

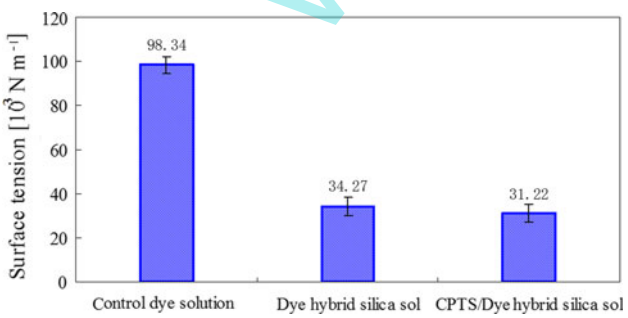

Fig. 3 Surface tension of silica sols

Contact angles

A water drop placed on the surface of cellulose matrix sinks into the cellulose matrix and disappears completely in 3 s as shown in Fig. 4a. After treated with CDHSS, the contact

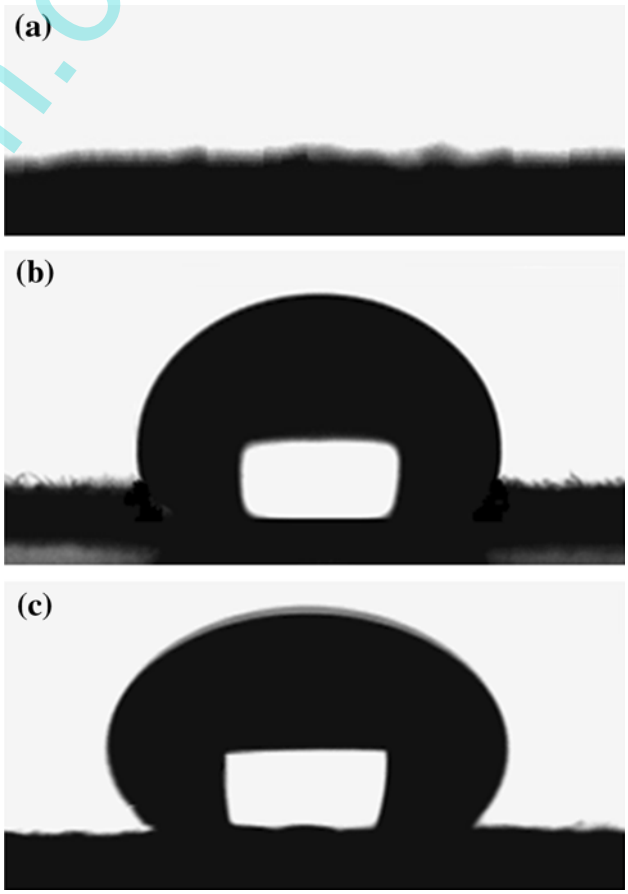

Fig. 4 Contact angles of coated samples: **a** control cellulose matrix, 0°; **b** DHSCCM, 112.35°; **c** CDHSCCM, 131.48°

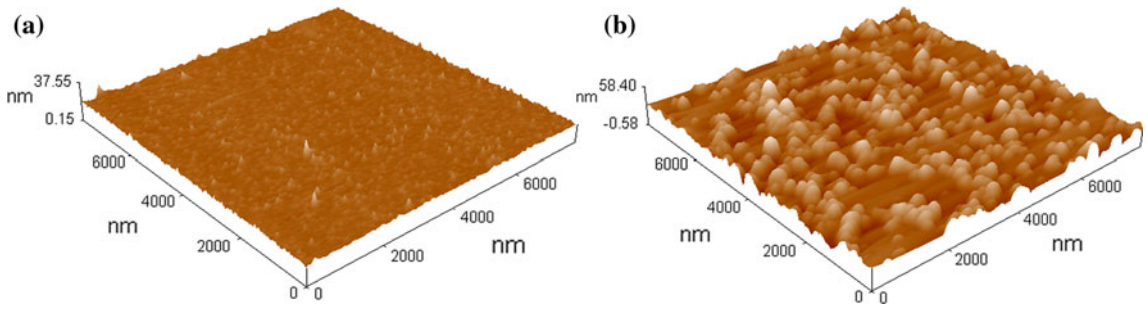

Fig. 5 The AFM images of the silica film surface treated with DHSS (**a**) and CDHSS (**b**)

angle of the matrix increases to 112.35° and is larger than the threshold 90°, which indicates that the cellulose matrix is hydrophobic. Via dehydrating and condensating reactions, the Si–O–Si chains are deposited on the surface of cellulose matrix [33]. Massive hydroxyl groups on the surfaces of cellulose matrix are enclosed by the silica coating, which contribute to hydrophobic property.

It is obviously observed that the water contact angle of cellulose matrix increases sharply from 112.35° to 131.48° after doped the CPTS in the DHSS (Fig. 4c), and the hydrophobic effect increases significantly. The wettability of matrix surfaces is affected not only by the chemical composition but also by the surface texture. The influence of CPTS brings an additional increase of the water contact angle, attributing to both of the long alkyl chloride aliphatic chain and the increased roughness of the coating surface.

Some reports have shown the surface topography of original cellulose matrix by AFM [34]. The surface texture of cellulose matrix expresses groove structure and natural distortion, whereas the roughness is not drastic, which has a slight effect on water repellency. From Fig. 5, two AFM images with significant difference micro-surface topographies are observed. The micro-surface coated with DHSS (Fig. 5a) is smooth, and only some weak peaks are displayed. By the Imager Statistical Analysis Software, the mean particle size, the mean height, the mean roughness, and the root mean square are 69.96, 20.30, 0.61, and 0.89 nm, respectively. While from Fig. 5b, a rougher micro-surface is presented. The mean particle size, the mean height, the mean roughness, and the root mean square are 140.74, 38.87, 4.20, and 5.36 nm, respectively. All these data are increased sharply. The mean particle size and height of the CPTS/dye hybrid silica film are larger than double of the dye hybrid silica film. The evident enhancement of the roughness (from 0.61 to 4.20 nm) is consistent with the changes of the contact angles (from 112.35° to 131.48°).

The effect of surface roughness on wettability can be explained by the Wenzel and Cassie–Baxter models. The basic assumption in Wenzel's theory is that the water drop penetrates the asperities, while the water drop suspends above the asperities for the Cassie–Baxter model [35]. After doped the CPTS, the crystal microtacticity of Si–O–Si is destroyed slightly. Besides the Si–O–Si formation, a new formation of Si–O–$(CH_2)_3$–Cl appears, which disturbs the original polymerization and brings new surface micro-topographies.

To further understand the hydrophobicity of the cellulose matrix, the wetting process of the cellulose matrix treated with CDHSS is analyzed (Fig. 6a).

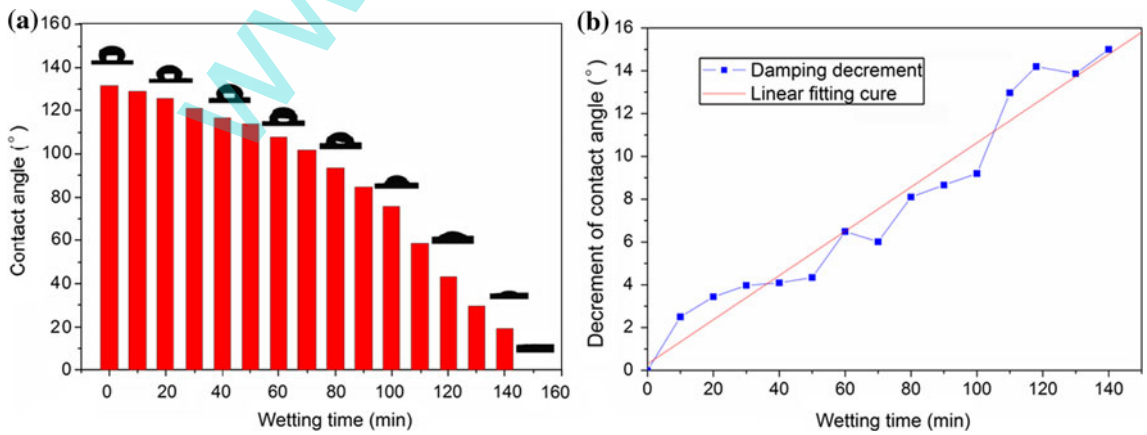

Fig. 6 Contact angles of water drop images on cellulose matrix treated with CDHSS (**a**) and the decrement cure of contact angle (**b**)

Table 1 Linear regression analysis

Parameter	Value	Error
A	0.30413	0.51936
B	0.10332	0.00633
Related coefficient	Standard deviation	Probability value
0.97647	1.05525	<0.0001

During the wetting process, the water drop wets the cellulose matrix gradually, and after approximately 150 min, the contact angle is near 0 (Fig. 6a). During this process, the decrease of contact angle is recorded every 10 min, and the damping decrement of the contact angle is analyzed. The 0° of the contact angle is difficult to accurately confirm for the irregular matrix surface and equipment constraint, so the time when the contact angle disappears is imprecise. The data do not count in the fitted cure.

From Fig. 6b, a linear equation is fitted,

$$y = A + Bx, \tag{3}$$

where y is decrement of contact angle (°), x is wetting time (min), and the parameter $A = 0.30413$ and $B = 0.10332$.

From Table 1, the related coefficient of the fitted linear equation is 0.97647 and the reliability is quite high. The probability value is <0.0001, and smaller than the threshold 0.01, which indicates that the fitted linear equation is highly significant and the fitted result is credible. Equation 3 shows that the decrement of contact angle is increased linearly with the wetting time, which primarily ascribes to the evaporation and diffuseness slowly at the surface and interior of the cellulose matrix.

Hydrostatic pressure

Figure 7 lists the hydrostatic pressures of the cellulose matrix coated with DHSS and CDHSS. It clearly indicates that the hydrostatic pressure of DHSCCM (3644.6 Pa) is significantly higher than that of the control-coated cellulose matrix (1939.4 Pa). The DHSS deposits on the matrix surface, and the coating decreases the porosity among the fibers. The increased compactability of the cellulose matrix contributes to preventing the H_2O passing through the matrix. The low surface-free energy decreases the penetrating capability of the H_2O.

After doped CPTS, the hydrostatic pressure of the cellulose matrix is improved to 4530.5 Pa (Fig. 7), increasing by 133.6 and 24.3% related to the hydrostatic pressures of control-coated cellulose matrix and DHSCCM, respectively. Besides improving the roughness of the fiber coatings, the alkyl chloride aliphatic chain in CPTS (Scheme 2) decreases the low surface-free energy of the coatings [36].

Color properties

The cellulose matrixes coated with control dye solution, DHSS, and CDHSS are measured, and the chromatic values, including *K/S*, *L**, *a**, *b**, *C**, and *h** are shown in Table 2. Compared with the control-coated cellulose matrix, the *K/S* values of the DHSCCM and CDHSCCM are 4.58 and 5.15, respectively. The results are mainly related to the surface tension of the solution (Fig. 4).

Table 2 Color properties of coated samples

Sample	*K/S* value	*L**	*a**	*b**	*C**	*h**
Control-coated cellulose matrix	3.95	54.94	42.58	16.95	45.83	21.71
DHSCCM	4.58	53.82	44.11	19.45	48.21	23.80
CDHSCCM	5.15	52.53	44.80	20.35	49.21	24.43

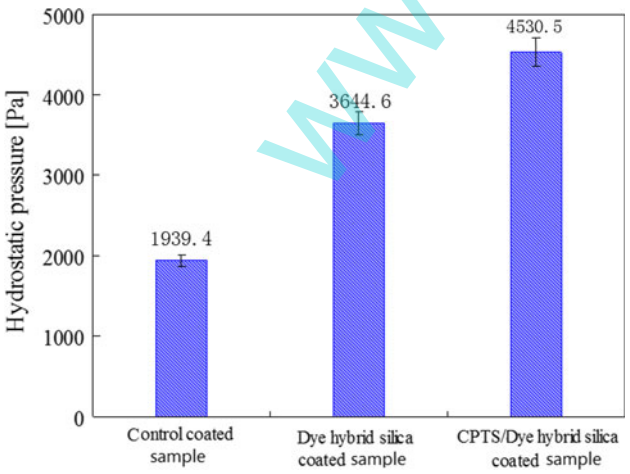

Fig. 7 Hydrostatic pressures of silica sol-coated samples

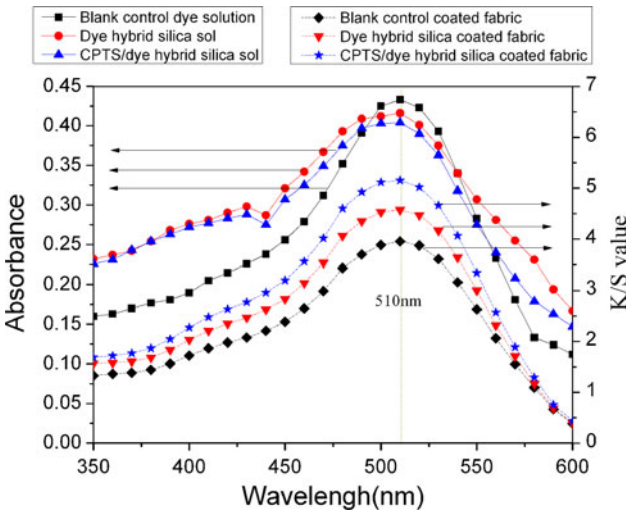

Fig. 8 Color properties of solutions and coated cellulose matrixes

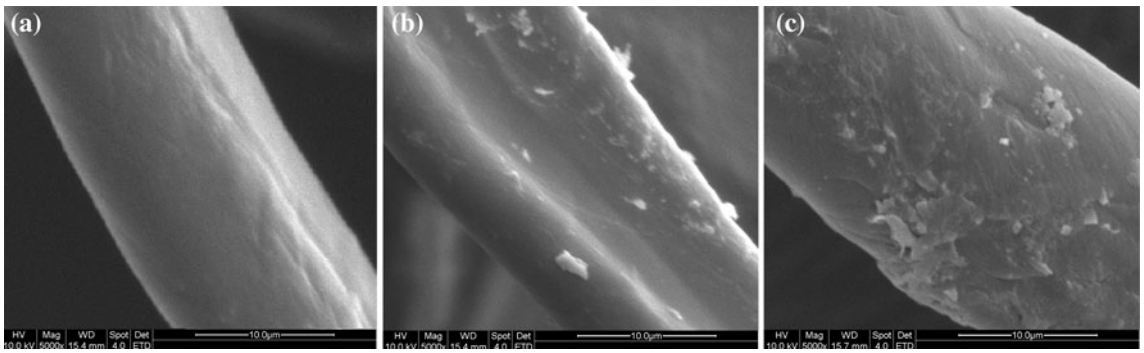

Fig. 9 SEM images of original cellulose matrix (**a**), coated cellulose matrix with DHSS (**b**) and CDHSS (**c**)

The surface tension of the control-coated solution is large (98.34×10^{-3} N m^{-1}), and the solution drop easily rolls down on the high speed turntable during spin-coating. Whereas, the surface tension of the DHSS is 34.27×10^{-3} N m^{-1} and the surface tension of the CDHSS is 31.22×10^{-3} N m^{-1}. The drop of the CDHSS wets more easily the cellulose matrix than the one without CPTS, so the dye molecules in the CDHSS solution are easily adsorbed to the cellulose matrix, leading to the increase of the *K*/*S* value.

From Table 2, the trend of color lightness L^* is opposite to the *K*/*S* value. The color chroma C^* of the CDHSCCM is the largest, which indicates that the color saturation increases slightly. Compared with the control-coated cellulose matrix, the hues (h^*) of the coated matrixes with and without CPTS increase by 9.6 and 12.5%, respectively. The maximum absorption wavelengths of the coated matrixes do not change and are coincident with the maximum absorption wavelengths of silica sols (510 nm) (Fig. 8). Nevertheless, the order of *K*/*S* values coated with different solutions is inconsistent with the absorbance of corresponding solutions. This result is attributed to the disparate polarities of solutions. In these solutions, the polarity of H_2O is the largest and the polarity of DHSS containing more ethanol is larger than that of the CDHSS. The color of direct red dye 4BS is aroused by $\pi \rightarrow \pi^*$ energy transition when the chromophore groups are irradiated. The ionization of the dye molecular increases in a solution with large polarity (such as H_2O), and the electric charge in the conjugated system easily transports, which increases the absorbance. However, when the dyes are adsorbed to the cellulose matrix and the solvents are evaporated, the effect of the solvent polarity disappears, and the *K*/*S* values are primarily involved to the content of the dyes (Fig. 3).

Surface morphology of cellulose matrixes

The surface of the uncoated cellulose matrix reveals characteristic parallel ridges (Fig. 9a), nevertheless after being coated with DHSS, such characteristics nearly disappear and dense silica nanoparticles coating appears on the surface of the cellulose matrix (Fig. 9b). The silica coating with a low surface-free energy brings about good hydrophobic property. After coated with CDHSS, the cellulose matrix coating with the modified silica nanoparticles still remains visible as shown in Fig. 9c [33, 37]. Besides the low surface-free energy, the modified silica nanoparticles bring to a rough micro-surface (Fig. 5b). The modified coating on the matrix surface benefits to the hydrophobic properties.

Conclusions

The CPTS in coatings acts in a specific role, and the remarkable hydrostatic pressure and contact angle attribute to the excellent adherence of the hybrid silica spin-coatings on cellulose matrix. From the SEM images, a continuous film is observed. The enhancement of film surface roughness generates an increased contact angle. The low surface tension improves the *K*/*S* value. The maximum absorption wavelengths of the coated matrixes do not change and are coincident with the maximum absorption wavelengths of silica sols (510 nm). The preparation of hydrophobic color matrix coated with silica sol doping dye will be a novel attempt on water-free dyeing in textile.

Acknowledgements This work is supported by the National Natural Science Foundation of China (20674031), the Business Doctoral Innovation Project of Jiangsu Province in China (BK2009672), the Graduate Students Innovation Project of Jiangsu Province in China (CX08S_016Z), the Fundamental Research Funds for the Central Universities (JUDCF09004) and the Excellent Doctoral Cultivation Project of Jiangnan University.

References

1. Costa SCS, Gester RM, Guimarães JR, Amazonas JG, Del Nero J, Silva SBC, Galembeck A (2008) Opt Mater 30:1432
2. Li PJ, Wu JH, Hao SC, Lan Z, Li QH, Huang YF (2011) J Appl Polym Sci 120:1752

3. Li YF, Zhang JH, Zhu SJ, Dong HP, Wang ZH, Sun ZQ, Guo JR, Yang B (2009) J Mater Chem 19:1806
4. Li X, Xiong RC, Wei G (2009) J Hazard Mater 164:587
5. Joshi M, Khanna R, Shekhar R, Jha K (2011) J Appl Polym Sci 119:2793
6. Huang WJ, Lee WF (2009) J Appl Polym Sci 111:2025
7. Sabzi M, Mirabedini SM, Zohuriaan-Mehr J, Atai M (2009) Prog Org Coat 65:222
8. Watanabe M, Tamai T (2006) Polym Chem 44:4736
9. Deshpande AV, Jathar LV, Rane JR (2009) J Fluoresc 19:607
10. Pardo R, Zayat M, Levy D (2009) J Mater Chem 19:6756
11. Davis SA, Burkett SL, Mendelson NH, Mann S (1997) Nature 385:42
12. Qin JQ, Zhao H, Zhu RQ, Zhang XY, Gu Y (2007) J Appl Polym Sci 104:3530
13. Karabela MM, Sideridou ID (2008) Dent Mater 24:1631
14. Khan MN, Al Dwayyan AS (2008) J Lumin 128:1767
15. Santiago JM, Keffer DJ, Counce RM (2006) Langmuir 22:5358
16. Lee WF, Yuan WY (2002) J Appl Polym Sci 84:2523
17. Yu MH, Gu GT, Meng WD, Qing FL (2007) Appl Surf Sci 253:3669
18. Yin YD, Alivisatos AP (2005) Nature 437:664
19. Aksit AC, Onar N (2008) J Appl Polym Sci 109:97
20. Morris CA, Anderson ML, Stroud RM, Merzbacher CI, Rolison DR (1999) Science 284:622
21. Parejo PG, Zayat M, Levy D (2006) J Mater Chem 16:2165
22. Schimidt H (2006) J Sol-Gel Sci Technol 40:115
23. Watanabe M, Tamaii T (2006) J Polym Sci A 44:4736
24. Morikawa T, Irokawa Y, Ohwaki T (2006) App Catal A 314:123
25. Rampazzo E, Bonacchi S, Montalti M, Prodi L, Zaccheroni N (2007) J Am Chem Soc 129:14251
26. Yin YJ, Wang CX (2009) Mater Res Innov 13:41
27. Tsai YS, Wang SH, Chen SY, Su SY, Juang FS (2009) Thin Solid Films 517:5338
28. Klomfar J, Součková M, Pátek J (2009) J Chem Eng Data 54:1389
29. Součková M, Klomfar J, Pátek J (2008) J Chem Eng Data 53:2233
30. Grundke K, Michel S, Knispel G, Grundler A (2008) Colloids Surf A 317:598
31. Yin YJ, Wang CX, Wang CY (2008) J Sol-Gel Sci Technol 48:308
32. Vince J, Orel B, Vilčnik A, Fir M, Vuk AŠ, Jovanovski V, Simončič B (2006) Langmuir 22:6489
33. Gao QW, Zhu Q, Guo YL (2009) Ind Eng Chem Res 48:9797
34. Vilčnik A, Jerman I, Vuk AŠ, Koželj M, Orel B, Tomšič B, Simončič B, Kovač J (2009) Langmuir 25:5869
35. Sánchez-Valencia JR, Blaszczyk-Lezak I, Espinós JP, Hamad S, González-Elipe AR, Barranco A (2009) Langmuir 25:9140
36. Huang PY, Chao YC, Liao YT (2006) J Appl Polym Sci 100:4711
37. Maity J, Kothary P, O'Rear EA, Jacob C (2010) Ind Eng Chem Res 49:6075